

Material characteristics of prefabricated concrete elements from a late 19th century church in lower Austria

FARKAS PINTÉR^{*,a} AND CHRISTOPHE GOSSELIN^b

^aScientific Laboratory, Federal Office for the Protection of Monuments, Arsenal 15/4, A-1030 Vienna, Austria

^bGeotest SA, En Budron E7, CH-1052 Le Mont-sur-Lausanne, Switzerland

* farkas.pinter@bda.at

Abstract

The late 19th century has preserved several important historic objects in the former Austro-Hungarian Empire made of Portland cement concrete. One of the most interesting examples of early concrete objects in Austria is the Parish church of Weissenbach an der Triesting near Vienna. The church was constructed between 1891 and 1893 using a novel double wall system: the inner wall was built from brick and the whole façade was covered with different prefabricated PC concrete elements.

The present study introduces the material characteristics of some of the original concrete elements at the church. Thin and polished sections of the samples were analyzed in the optical and scanning electron microscope in order to determine the properties of the cement and aggregates. Façade elements, such as ledges, show a double-layered structure: a dense outer layer is followed by a porous tamped concrete layer to lighten the element. Composition and grains size of unhydrated clinker phases and the presence of solid fuel remnants suggest the use of a shaft kiln, inhomogeneous raw meal, firing conditions and slow cooling rates. Differences in the microporosity between the two layers refer to different w/c-ratios during the production of materials. SEM-EDX measurements and element ratio plots highlight the composition and change in the binder due to the interaction of cement hydrate phases, aggregates, and atmospheric pollutants.

Additionally, dolomite aggregates exhibit the phenomenon of dedolomitization, manifesting in the transformation of $\text{CaMg}(\text{CO}_3)_2$ grains into calcite and brucite. The phenomenon, however, is not connected with the formation of alkali-silica gel, thus it is harmless and cannot be classified as deleterious ACR.

Keywords: Portland cement, historic concrete, clinker phases, optical microscopy

I. INTRODUCTION

Portland cement was first produced in 1856 as natural cement in Austria. The last decades of the 19th century, however, were dominated by the use of Roman cements as hydraulic binders (Zehetner, 2010). At the turn of the 20th century this trend rapidly changed and the success story of Portland cement has begun in the Austro-Hungarian Empire. Some of the most interesting applications of Portland cement in Eastern Austria were connected to the talented Austrian engineer Adolf Freiherr von Pittel (1838-1900). In the 1870s he established several cement plants near Vienna, where hydraulic lime and Roman cement were produced, but he promptly completed his array of products with prefabricated casts and artificial stones made from Portland cement (Heimel et al, 2010). Pittel's success resulted not only in the good quality hydraulic binders he produced, but also in the widely distributed prefabricated products (Figure 1) in the

Austro-Hungarian Empire and some exclusively managed patents in the field of concrete technology (Heimel et al., 2010).

One of Pittel's main creations was the Parish church in Weissenbach an der Triesting (Lower Austria, Figure 2), which he donated to his community. It was constructed between 1891 and 1893 using a double wall system: the inner wall was built from brick and the whole façade was covered with prefabricated PC concrete elements (Heimel et al, 2010). The present study is a part of an international cooperation aimed at studying the 19th century concrete buildings within the territory of the former Austro-Hungarian Empire.

Due to the abundance of large unhydrated cement grains and non-carbonated cement paste in the samples, the paper focuses on the chemical-mineralogical characterization of residual clinker phases and hydration products, attempting to determine the original composition, characteristics, and production techniques of the cement and concrete.

Preisblatt für Cementwaren A/VII.

Gusswaren aus Portland-Cement-Beton.

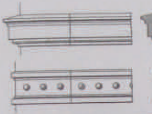

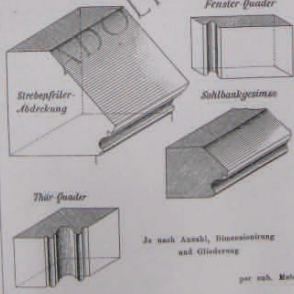
Verf. Part. Nr.	Gegenstand	Gewicht in Kilogr.	PREIS			Anmerkung
			Runde	per-cm. Nr.	Stk.	
31	Gurt- und Bandgesimse 	per cub. Meter	2400	—	50	Werden nur auf Bestellung ausgeführt und geliefert.
32	Säulenschäfte, Säulentrömmeln 	per cub. Meter	2400	—	55	
33	Werkstücke für Kirchen. Fensterquadern  Sakelbankgesimse Thürquadern Je nach Anzahl, Dimensionierung und Gliederung per cub. Meter	2400	—	50-60	Solche Arbeiten werden in der Regel nur an Ort und Stelle zu machen sein. Die Lieferung erfolgt genau nach Zeichnung. Die schillernden Flächen der Werkstücke werden dem Abnehmer durch poliert.	

Figure 1: Examples from Pittel's catalog (1890s) containing precast concrete elements (courtesy of the Country Museum, Weissenbach a.d. Triesting).

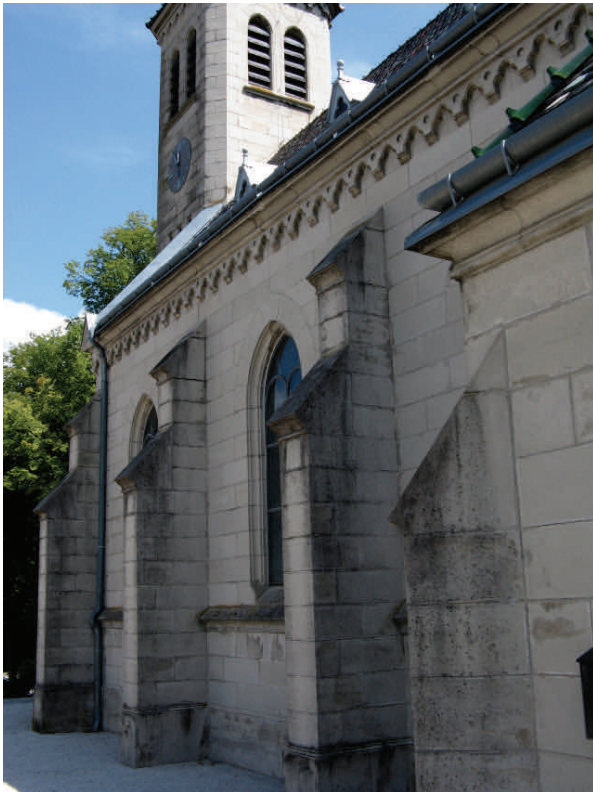


Figure 2: The western façade of the Parish church of Weissenbach a.d. Triesting.

II. SAMPLING AND ANALYTICAL METHODS

Two samples, one from a slightly damaged ledge (WB-1) at the western façade (Figure 2) and another concrete fragment from the socle (WB-2) on the southern side, were taken for analyses. Thin and plane sections prepared from the samples were etched with Nital (1.5 ml of HNO_3 in 100 ml of isopropyl alcohol; Campbell 1999) for 7 to 9 seconds and analyzed in the optical microscope (Zeiss AXIOScope A1) using reflected and transmitted polarized light. Depending on the reactivity of the cement phases, alite normally turned blue to tan; belite was brown to blue and both phases showed details of internal structure (Campbell, 1999). Phases of the interstitial matrix (C_3A and ferrite) were light gray and white in color. Non-etched polished sections were coated with carbon and analyzed in the scanning electron microscope (SEM, Zeiss EVO MA 15), coupled with an energy dispersive X-ray spectrometer (EDS, Oxford DryCool, 15kV, 300 pA). A number of standardized point analyses were used to characterize the chemical composition of the binders.

III. RESULTS AND DISCUSSION

General features of the concrete samples

Based on macroscopical observations on broken surfaces (Figure 3), samples exhibited compact structure; material loss due to weathering could not be observed. By the use of phenolphthalein on fresh fracture surfaces an intensive purple discoloration (Figure 3) at ca. 0.5 to 1 cm from the surface indicated the preserved alkalinity of the binder. This phenomenon suggests adequately low capillarity, probably due to a relatively low w/c ratio of the fresh concrete (Idorn & Thaulow, 1983). On the contrary to this, the more porous tamped concrete layer (Figure 3) in the sample WB-1 did not show any discoloration with effect from the phenolphthalein test, which suggests higher capillary porosity and the influence of carbonation and/or leaching on the cement paste, due to contact with air and humidity along e.g. fitting gaps on the façade.

Optical microscopy

Confirming the phenolphthalein test, the high birefringence of the matrix in the sub-surface zones corresponds to carbonated binder portions. Estimated water to cement ratios being 0.4-0.45 (outer concrete, Figure 4, WB-1) and ~ 0.50 for the sample WB-2 (Figure 5). The sample WB-1 contained many irregularly shaped compaction pores (Figure 4), while the sample WB-2 had very few entrapped air voids (1 to 2 vol.%, Figure 5). The cement paste of both samples were free of any cracks.

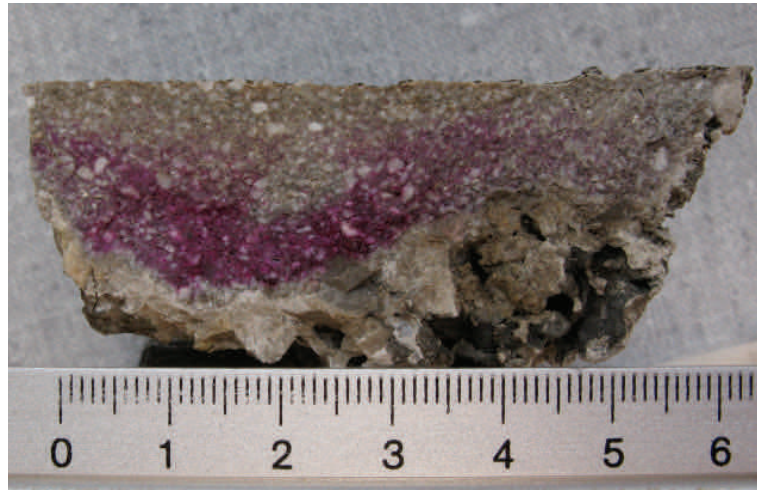


Figure 3: Alkaline binder portions highlighted by using phenolphthalein test on the broken surface of the sample. Below the discoloration the cement paste of the tamped concrete containing large aggregates was fully carbonated WB-1 (precast ledge).

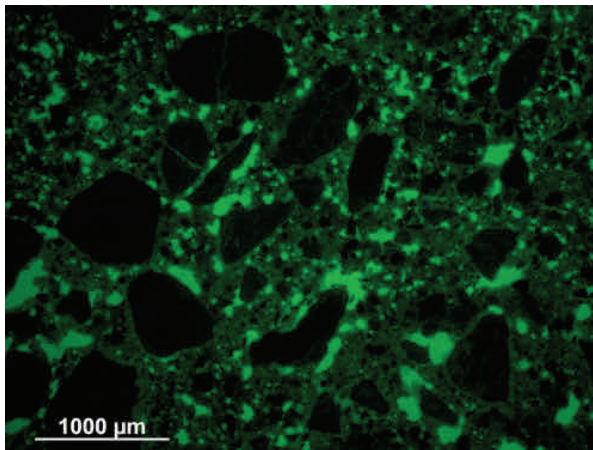


Figure 4: High amounts of compaction pores and low to moderate w/c ratio of the non-carbonated cement paste in the sample WB-1 (thin section, UV microscopy).

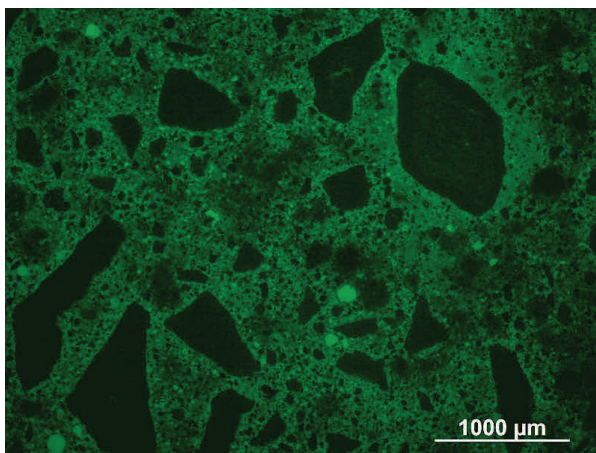


Figure 5: The compact cement paste exhibits slightly inhomogeneous capillary porosity and contains few rounded air voids (WB-2, thin section, UV microscopy).

The most characteristic feature of both samples is a large amounts of very coarse residual cement particles, exhibiting a maximum of 0.9 and an average diameter of 0.2 to 0.3 mm (Figures 6 to 11), typical for historic PC mortars and concretes (Idorn & Thaulow, 1983; Blezard, 1984, Weber et al, 2012).

A significant portion of cement grains have remained unhydrated (Figures 6 to 11). Traces of hydration could mainly be observed on the margins of the residual phases. Due to the higher w/c ratio the inner concrete layer of the sample WB-1 exhibits higher degree of hydration.

The aggregate contained in the mortars at grain sizes of 0.1 to 3 mm (WB-1) and 0.1 to 4 (WB-2) is exclusively of crushed dolomite; the estimated binder to aggregate ratio being 1 to 2.5-3 (WB-1) and 1 to 4 (WB-2) with a definitely higher amount of fine fraction (0 to 0.05 mm) in the sample WB-2, which probably also had an impact on the higher water demand and thus higher capillary porosity of the mortar (*cf.* Figures 4 and 5).

Characteristics of cement phases

Residual cement grains that entirely or partly survived the hydration and later carbonation were used to determine the composition and properties of the original cement. In terms of composition and grain size of single crystals, cement grains exhibited very inhomogeneous features. Interpretation of the observations was based on Insley (1936), Gille et al (1965), Idorn & Thaulow (1983), Blezard (1984), and Campbell (1999).

Alite

Residual cement grains contain large amount of unhydrated euhedral to subhedral, partly distorted C_3S (Figures 7, 8 and 10). The size of single crystals

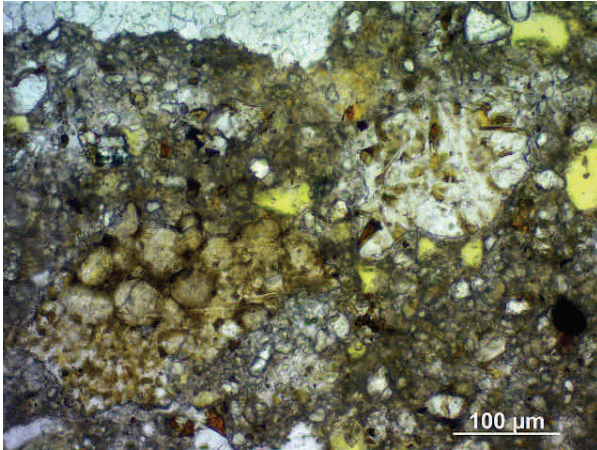


Figure 6: Coarse unhydrated belite nest (center left) and another residual cement grain (center right). WB-1, thin section, plane-polarized light.

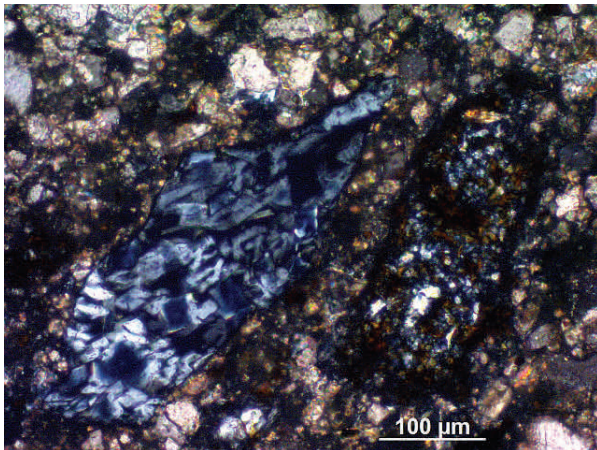


Figure 7: Large non-hydraulic cement grain made up of platy gehlenite crystals (center left, grayish blue) and a partly hydrated residual cement grain containing small belite and euhedral C_3S crystals (center right). WB-2, thin section, cross-polarized light.

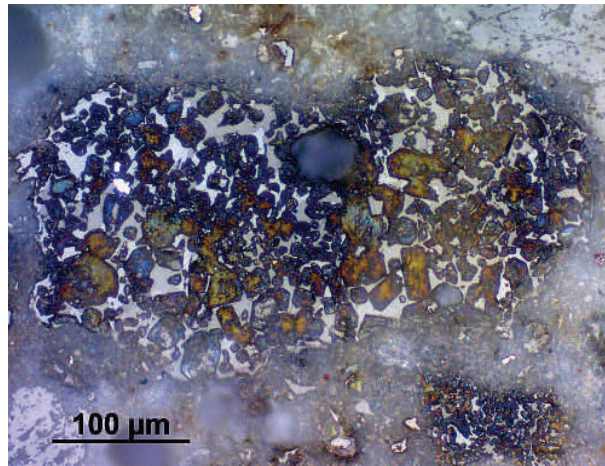


Figure 8: Large residual cement grain containing angular alite (tan) and rounded belite (blue) crystals. Interstitial phases are made up of aluminates (grey) and ferrite (white). WB-1, reflected light, Nital etching.

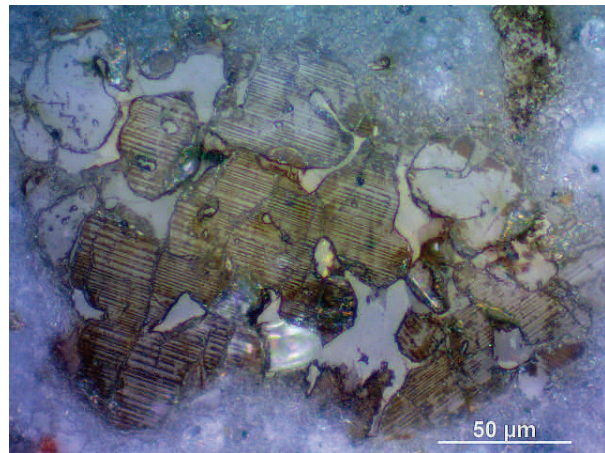


Figure 9: Large residual cement grain containing Type II belite (brown) and C_3A as flux. WB-1, reflected light, Nital etching.

varies between 5 and 80 μm (average 20 to 50 μm). Alite mostly contains small residual belite nuclei (e.g. Figure 8). Several crystals show corroded surfaces and marginal decomposition into belite (Figure 10). This latter observation indicates slow rates of cooling, while the different sizes of alite can also be explained by an inhomogeneous raw meal and/or inhomogeneous firing conditions in the kiln.

Belite

Belite shows round to angular, often atypical or distorted shapes. Its crystal size varies within a wide range of 5 to 100 μm , though single crystals around 20-30 μm are frequent (Figures 7 and 9). Up to 0.6 mm large nests of coarse, spherical C_2S with very little interstitial material suggest concentration and inhomogeneities of quartz in the raw feed.

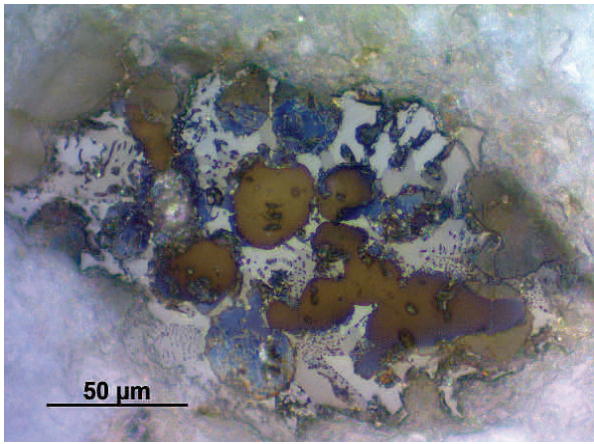


Figure 10: : Distorted alite crystals (brown) showing decomposition into belite (small blue crystals) on their margin in coarse grained flux phases. WB-2, reflected light, Nital etching.

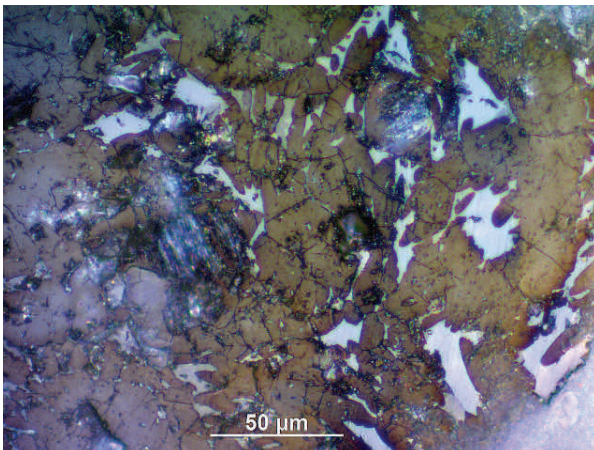


Figure 11: Belite (brown) showing segmented fingerlike extensions into the a coarse crystalline ferrite-rich matrix (white). WB-1, reflected light, Nital etching.

Segmented fingerlike sections (Figure 11) were observed both in thin and polished sections, referring to slow cooling and eventually to reducing conditions. Identical features were reported by Idorn & Thaulow (1983) and Blezard (1984) on a historic PC (Aspdin's cement) from 1850, burned in a shaft kiln. Very small belite droplets (Figure 11) could frequently be observed as inclusions within C_3A , due to slow cooling where excess silicates crystallized from the flux (Gille et al., 1965). The lamellar structure of the larger C_2S crystals can easily be observed in transmitted light or after the structural etching in reflected light. The predominant types are crystals with two or more sets of intersecting lamellae (Type I, Insley, 1936), as well as irregular grains with one set of parallel lamellae (Type II, Insley, 1936, Figure 9).

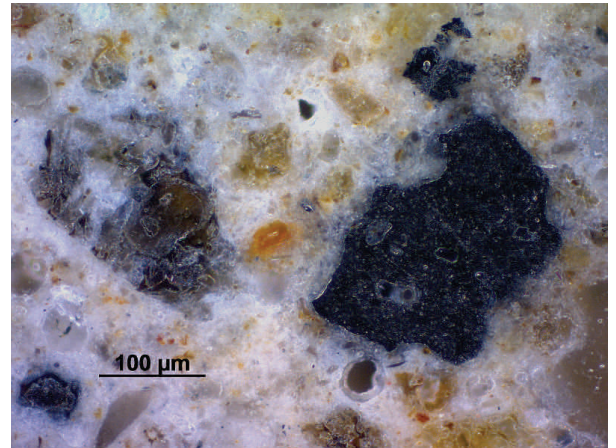


Figure 12: Large residue of solid fuel (right). WB-1, reflected light, dark field.

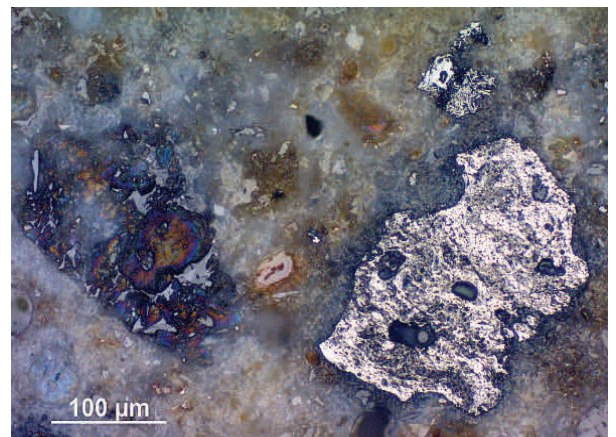


Figure 13: The same grains as in the Figure 12 containing anisotropic graphite crystals. Cross-polarized reflected light.

Aluminate and ferrite

Flux phases such as C_3A and Ca-Al-ferrite form very coarse, large and well-developed crystals (Figures 8, 9 and 11). These features are also consequence of a slow cooling rate.

Remnants of solid fuel and miscellaneous phases

Black, shard-like (Figure 12), in transmitted light opaque inclusions, in average of 50 to 500 μm of diameter, can be classified as solid fuel remnants. Observations in reflected cross polarized light proved the anisotropic nature of phases, suggesting the presence of graphite in the organic matter (Figure 13).

Apart from the PC cement clinker phases described above, the samples contain small quantities of other components indicating inhomogeneous firing conditions in the kiln. The most frequently observed phase is gehlenite (C_2AS) exhibiting platy shaped crystals of first order gray interference color (cf. Figure 7).

Dedolomitization of aggregates

Small amounts of the crushed dolomite sand used as aggregates shows dedolomitization in both concrete elements. The reaction products are mainly restricted to the outer rim of some of the grains, but decomposition along cracks was also observed (Figure 14). Evidence of dedolomitizations are small rims of brucite ($Mg(OH)_2$) and calcite (Figure 14) in the zones of interaction. The process itself has not produced expansion because no cracks originated from the dedolomitized aggregate into the cement paste were observed. The so-called deleterious alkali-carbonate-reaction (ACR) is made up of two reactions; the alkali-silica-reaction (ASR) occurs between the alkali-rich pore solution and micro- or cryptocrystalline SiO_2 as impurity in the dolomite stone and the above described dedolomitization (Katayama, 2010; Grattan-Bellew et al, 2010), which indicates the reaction between the high alkali pore solution and the $CaMg(CO_3)_2$. Former extensive research (Katayama, 2010) has shown that expansive forces do not happen upon dedolomitization. If expansion and formation of cracks, which reach the cement paste, are observable, the damage is always connected to ASR. Since neither microcrystalline SiO_2 in the dolomite aggregates, nor alkali-silica gel have been detected in the vicinity of the dedolomitized areas, the observed marginal decomposition of the aggregates cannot be classified as ACR.

Chemical composition of the binders

The elemental composition of hydration products, measured by EDS, according to the phenolphthalein

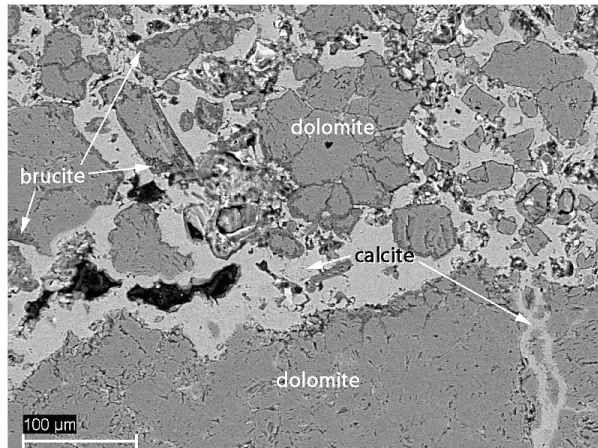


Figure 14: Marginal dedolomitization of dolomite aggregates into brucite and calcite. WB-1, SEM-BSE.

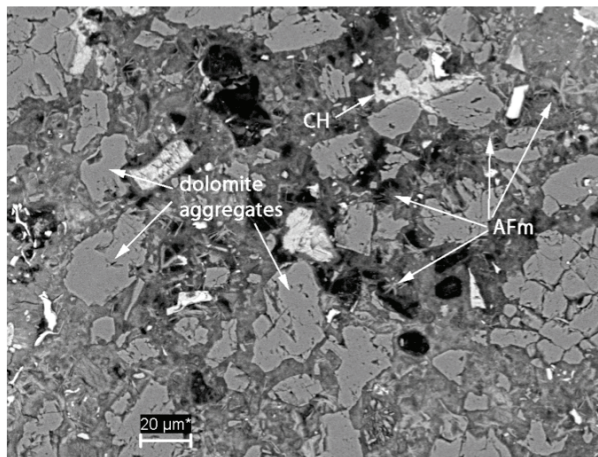


Figure 15: Fine grained dolomite aggregates, portlandite and AFm phases (probably monocarboaluminate). WB-2, SEM-BSE.

test, on the non-carbonated zone of the matrix, has been expressed in atomic ratio plots Ca , Si , Al and S .

Si/Ca vs. Al/Ca plots (Figures 16a and 17a) of both samples show the presence of different fine grained AF_t (ettringite) and AF_m phases. Furthermore, the Si/Ca ratio of the inner C-S-H indicates, especially in the sample WB-2 (Figure 17b; yellow ellipse), higher values than those of the theoretical Si/Ca ratio (0.58) given as a reference for pure synthesized $C_{1.7}SH$. This difference may be explained either by partly decalcified $C-S-H$ and/or by the influence of the clay fraction in the raw materials and subsequent clinker. The presence of portlandite confirms the alkaline environment in the binder.

Values plotted in the Al/Ca vs. S/Ca plots (Figures 16b and 17b) confirm the nature of AF_m phases. In the sample WB-1 (Figure 16b) the main AF_m phase is monosulphate, coexisting probably also with some minor amount of monocarbonate, as suggested by the dots marked by the red ellipse. In the sample WB-2 monosulphate is completely replaced by monocarboaluminate, as characterized by the values 0.15 to 0.4 (Al/Ca) and 0.02 to 0.05 (S/Ca). The presence of monocarbonate can be explained by the high amounts of fine grained carbonate (dolomite) filler, which has partly reacted during hydration with the aluminate phases.

There is a considerable amount of sulphate-bearing phases in both samples, which suggests the presence of primary Ca-sulphate in the cement. Historical data (Riepl, 2008) show that since 1889 the Association of Austrian Cement Plants allowed a maximum gypsum content of 2% in PCs, which can be interpreted as a deliberately admixed additive. However, the use of a solid fuel containing natural SO_3 -bearing phases (Michaelis, 1869) and its effect on the clinker composition (e.g. larger amount of alkali-sulphates formed during firing) as well as on hydrate phases cannot be excluded.

The effect of excess sulphate is suggested by the atomic ratio plots. External SO_3 has reacted with monosulphate to produce secondary ettringite, which could also be detected as secondary pore fillings or sometimes in the form of reactivated C_3A around unhydrated residual cement. A crack pattern due to expansive forces cannot be seen.

IV. CONCLUSIONS

Using reflected and transmitted polarized light microscopy, completed with SEM-EDS measurements on polished and thin sections, the composition and material characteristics of two historic, pre-fabricated PC concrete elements from the Parish church in Weissenbach an der Triesting, dating back to 1893, were carried out. The low to moderate w/c ratio and the use of historical grinding tech-

niques have induced the preservation of several unhydrated residual cement grains in the samples. These residual grains contained all four main PC phases; their relative amount, crystal size and shape suggested, however, different burning and cooling conditions and raw feed composition in comparison with modern PC clinkers. Features such as inhomogeneous crystal sizes of alite exhibiting frequently decomposition into belite on its margin, fingerlike sections of belite and coarse crystalline flux phases suggest slow cooling rates and eventually also reducing conditions during the calcination process. Due to the coexistence of the different belite types, uneven kiln temperatures and cooling rates, typical for shaft kilns, can be assumed. Beside the aforementioned observations, for modern PC atypical clinker phases containing C_2AS and probably also other low temperature, non- or slightly hydraulic Ca-(aluminate)-silicates also suggest inhomogeneous heat distribution during firing. Small fragments of graphite-bearing inclusions indicate the use of a solid fuel.

Crushed dolomite sand used as aggregate in both concrete elements exhibited partly dedolomitization on marginal zones and along cracks. The reaction, however, is not connected with the formation of ASR, thus it is harmless and cannot be defined as alkali-carbonate reaction.

Binder portions with preserved alkalinity enabled to determine the nature of hydration products based on the chemical composition of the cement paste. Although the formation of secondary ettringite from monosulphate due to excess SO_4^{2-} rather suggests the use of Ca-sulphate as setting retarder admixed to the cement, the effect of sulphur-rich fuel producing alkali-sulphates in the clinker phases during firing cannot be excluded either. One of the samples clearly indicated the effect of the fine-grained carbonate aggregate portion on the hydration products: monosulphate was replaced by monocarboaluminate. In the other sample monosulphate coexisted with some minor amount of monocarbonate.

Based on the extensive investigations of the samples it can be concluded, that the cement used for producing the concrete elements was burned in a shaft kiln above the sintering temperature, but still under inhomogeneous heat distribution, with probably long residence time, slow cooling rates and inhomogeneous raw feed. Chemical data of the cement paste suggests the use of artificially admixed Ca-sulphate as a setting retarder.

The factors such as the w/c-ratio, grading curve of the aggregates and the partial reaction of the sand particles with clinker phases during the hydration have played an important role in a remarkable performance of the concrete cast elements during the last 120 years.

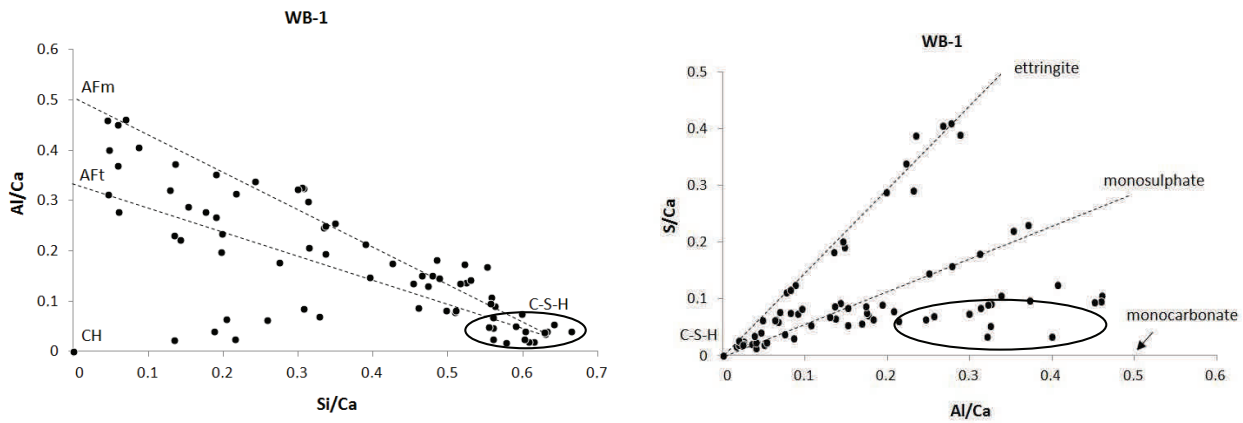


Figure 16: a) Si/Ca vs. Al/Ca plot of the X-ray data (WB-1), b) Al/Ca vs. S/Ca plot of the X-ray data (WB-1).

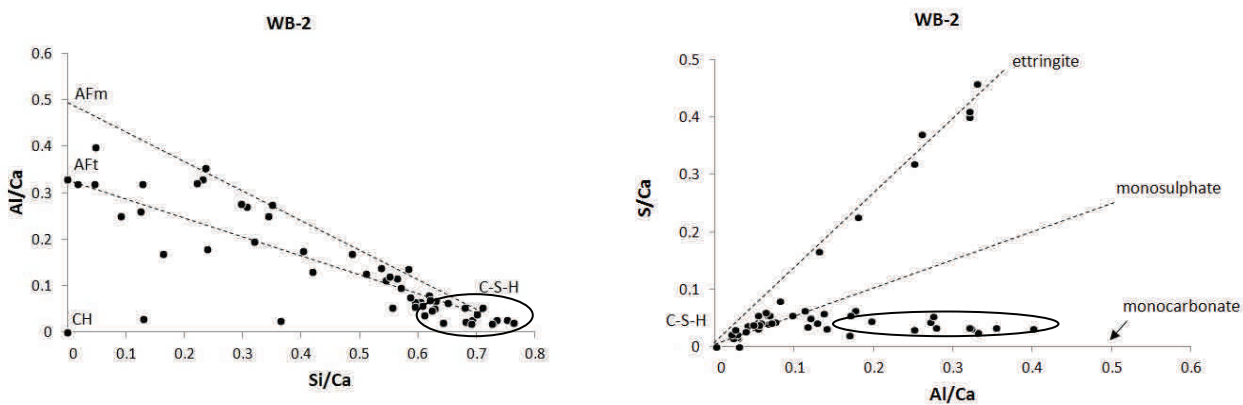


Figure 17: a) Si/Ca vs. Al/Ca plot of the X-ray data (WB-2), b) Al/Ca vs. S/Ca plot of the X-ray data (WB-2).

ACKNOWLEDGEMENT

The authors would like to thank to Mr. Helmut Heimel (Weissenbach an der Triesting) for supporting the sampling and providing valuable information about the history of the object.

REFERENCES

- Blezard, R.G. (1984): "A discussion of the Paper "Examination of 136-Years-Old Portland Cement Concrete," by G.M. Idorn and N. Thaulow". *Cement and Concrete Research*, Vol. 14, pp. 154-156.
- Blezard, R.G. (2004): "The history of calcareous cements". In: (Hewlett, P.C. ed.) *Lea's chemistry of cement and concrete*. 4th Edition, Elsevier, pp. 1-21.
- Campbell, D.H. (1999): "Microscopical Examination and Interpretation of Portland cement and Clinker". 2nd Edition, *Portland Cement Association*, USA, 201p.
- Gille, F., Dreizler, I., Grade, K., Krämer, H., Woermann, E. (1965): "Mikroskopie des Zementklinkers, Bilderatlas". Association of the German Cement Industry, *Beton-Verlag*, Düsseldorf, West Germany, 75 p.
- Heimel, C., Heimel, H., Schicht, P. (2010): "Frühe Betonfertigteile in Niederösterreich – Freiherr von Pittel und die Kirche von Weissenbach an der Triesting". In: G. Lindner (Ed.), *Denkmalpflege in Niederösterreich*, Band 43: *Beton*, pp. 42-45.
- Idorn, G.M., Thaulow, N. (1983): "Examination of 136- Years-Old Portland Cement Concrete". *Cement and Concrete Research*, Vol. 13, pp. 739-743.
- Insley, H. (1936): "Structural Characteristics of Some Constituents of Portland Cement Clinker," *Journal of Research of the National Bureau of Standards*, Vol. 17, Research Paper RP917, Washington, D.C., pp. 353-361.
- Grattan-Bellew P.E., Mitchell L.D., Margeson J., Min, D. (2010): "Is alkali-carbonate reaction is just a variant of alkali-silica reaction ACR=ASR?". *Cement and Concrete Research*, Vol. 40, pp. 556-562.
- Katayama, T. (2010): "The so-called alkali-carbonate reaction (ACR) – Its mineralogical geochemical details, with special reference to ASR". *Cement and Concrete Research*, Vol. 40, pp. 643-6751.
- Michaelis, W. (1869): „Die hydraulischen Mörtel insbesondere der Portland-Cement in chemisch - technischer Beziehung für Fabrikanten, Bautechniker, Ingenieure und Chemiker“. - *Verlag von Quandt & Händel*, Leipzig S. 315 p.
- Riepl, F. (2008): "Die wirtschaftliche und technologische Entwicklung der Zementindustrie unter besonderer Berücksichtigung der Verdienste von Hans Hauenschild". Unpublished doctoral thesis, Universität Wien, 140 p.
- Weber, J., Bayer, K., Pintér, F. (2012): 19th century 'novel' building materials: examples of various historic mortars under the microscope". In: J. Válek, J. J. Hughes, C.J.W.P. Groot (Eds.), *Historic mortars- Characterization, Assessment and Repair*, RILEM 7, Springer, pp. 89-103.
- Zehetner, K. (2010): "Zementwerke in Niederösterreich". In: G. Lindner (Ed.), *Denkmalpflege in Niederösterreich*, Band 43: *Beton*, pp. 201-21.